Void Detection in Grouted Post-tensioned Bridges Using Time Domain Reflectometry

Michael Chajes, Professor and Chair[1]
Department of Civil & Environmental Engineering
301 DuPont Hall
University of Delaware
Newark, DE 19716
Voice (302) 831-6056
Fax (302) 831-3640
chajes@ce.udel.edu

Robert Hunsperger, Professor
Department of Electrical & Computer Engineering
214 Evans Hall
University of Delaware
Newark, DE 19716
Voice (302) 831-8031
Fax (302) 831-4316
hunsperg@ee.udel.edu

Wei Liu, Post Doctoral Fellow
Center for Innovative Bridge Engineering
University of Delaware
Newark, DE 19716
Voice (302) 831-0678
Fax (302) 831-4316
wliu@ee.udel.edu

Jian Li, Graduate Assistant
Department of Electrical & Computer Engineering
University of Delaware
Newark, DE 19716
Voice (302) 831-0678
Fax (302) 831-4316
jian@mail.eecis.udel.edu

Eric Kunz, President
Vetek Systems Corporation
6 Oak Road
Elkton, MD 21921
Voice (410) 398-7131
VETEKsys@aol.com

---

[1] Corresponding Author

ABSTRACT

The presence of voids is a serious problem in grouted post-tensioned bridges because voids greatly reduce the corrosion-protective capabilities of the grout. Current methods for void detection suffer several significant drawbacks. A new method utilizing time domain reflectometry (TDR) is discussed in this paper. TDR is a well-developed method for detecting discontinuities in electrical transmission lines. A recent study has shown that TDR can be used as an effective nondestructive damage detection method for concrete bridges. A void changes the electrical properties of transmission lines and therefore introduces electrical discontinuities. It can be detected and analyzed by TDR. Experiments on short specimens that are used to model grouted post-tensioning ducts with built-in voids have been conducted and demonstrate the potential of TDR as a void detection method.

INTRODUCTION

Void detection is an important aspect of nondestructive evaluation of post-tensioned concrete bridges, as the presence of a void leaves a section of post-tensioning strands vulnerable to corrosion. Both the US and the UK have developed significant concerns regarding the condition of post-tensioned segmental concrete bridges. The problem revolves around the fact that it is difficult to ensure complete grouting of post-tensioning tendons. When post-tensioned ducts are not completely grouted and voids are present, the steel tendons are left vulnerable to premature corrosion (1). This very issue led to the declaration of a moratorium on the construction of post-tensioned bridges by the UK's Department of Transport in 1992 (2).

More recently, distress and failure of post-tensioning tendons due to inadequate grouting were found in Florida on the Mid-Bay Bridge. These problems were reported in a preliminary report issued by the Florida Department of Transportation on February 8, 2001 (3). The report states that "on August 28, 2000, during a routine inspection of the Mid-Bay Bridge, a post-tensioning tendon in Span 28 was observed to be significantly distressed." The discovery "led to an immediate *walk-through* inspection to verify if other post-tensioning tendons were exhibiting similar signs of distress. A post-tensioning tendon in Span 57 was found completely failed at the north end of the tendon as evidenced by pull out of the tendon from the expansion joint diaphragm." Subsequent examination of the two distressed/failed tendons revealed that "the condition of the grout for these two tendons was suspect. Air cavities, bleed water trails and soft, chalky grout characteristics were observed." The report goes on to say that "significant voids in grout or a highly porous grout can reduce the corrosion protective capabilities of this system … (and) there is a consistent presence of voids in the tendons." Figure 1 shows a typical post-tensioning tendon and the location at which voids (and resulting tendon failures) were found in the Mid-Bay Bridge.

While it is well known that incomplete grouting of ducts (i.e., voids) can leave tendons vulnerable to corrosion (1,2,3), effective and economical methods for detecting voids in post-tensioning ducts are not readily available. While some void inspection methods, such as bore scope, impact-echo, and ground-penetrating radar inspections, do exist, each has its drawbacks.

In order to perform a bore scope inspection, a hole is drilled on the grout element and a flexible bore scope is inserted. A still image or video can be captured through the bore scope. However, this is not a nondestructive method, and it may affect the long-term integrity of the structure.

The basic principle of the impact-echo technique is that a stress pulse is introduced into the structure from an impact source, such as a hammer or ball drop. The resulting stress waves are monitored by an ultrasonic transducer also on the surface of the structure. These stress waves travel back and forth between the surface and the voids that may exist in the structure. By observing the resonant frequency, the distance from the surface to the void can be determined. Impact-echo techniques have been shown to be fairly effective for locating large voids. However, smaller voids are difficult to detect with this technique due to the relatively low frequencies involved.

In a test using ground-penetrating radar, a high-frequency electromagnetic wave is emitted via an antenna into the structure under evaluation. When the wavefront encounters an interface where the electromagnetic properties change, a portion of the wave reflects at the interface. The reflected wave is detected by a receiver antenna and analyzed. However, in order to obtain a usable signal, the antenna needs to be placed within very close proximity to the concrete structure. Meanwhile, the presence of reinforcing steel will greatly disturb the radar image. Voids behind the steel will not detectable because the emitted wave will not penetrate metal of a reasonable thickness.

Other advanced methods have also been used to detect corrosion and voids. However, they have met with limited success due to the skill needed to analyze the data as well as the expense of the equipment.

To help ensure that new post-tensioned, segmental concrete bridges will not prematurely deteriorate, which could result in major economic losses as well as potentially threatening the safety of the traveling public, new NDE methods are needed to ensure proper grouting in post-tensioned applications. This paper describes research conducted in an effort to develop such a method. Specifically, a novel and economical nondestructive evaluation technique using time domain reflectometry (TDR) is demonstrated. TDR is an electrical measurement technique that has been used since the 1940s to determine the spatial location and nature of faults in transmission lines (4). It involves sending an electrical pulse along a transmission line and using an oscilloscope to observe the echoes returning back from the device under test. The embedded steel cable can be modeled as an asymmetric, twin-conductor transmission line by applying a sensor wire along with the cable (5). Physical defects of the cable or the grout surrounding the cable will change the electromagnetic properties of the line and can be detected by TDR.

This paper focuses on the use of the TDR method to detect voids in grouted post-tensioning ducts. TDR was successfully used as a void detection method for several laboratory specimens. While this particular application of TDR has not been implemented in the field, the effectiveness of TDR for corrosion detection has been verified through both small-scale laboratory tests (6) and field demonstration (7).

TWO-WIRE TRANSMISSION LINE MODEL

TDR was introduced recently as a corrosion detection method for post-tensioning strands by applying a sensor wire alongside the steel strand to establish an asymmetric two-conductor transmission line. For a thorough analysis of the wave propagation in this transmission line, one needs to solve Maxwell's equations with boundary conditions imposed by the physical nature of the strand and surrounding grout. For simplicity, a distributed parameter model is used to study the wave propagation in this transmission line. Wave propagation is described in terms of voltage and current by utilizing the equivalent circuit shown in Figure 2.

The distributed parameters of the steel strand transmission line are calculated from the geometry and material parameters of the strand. The capacitance per unit length is calculated by considering the electric field of two parallel infinitely long straight line charges of equal and opposite uniform charge densities. The equipotential surfaces are cylinders with axes parallel to the line charges. The capacitance per unit length of the line is obtained by placing the two conductors in two equipotential surfaces, and calculating the potential difference. The inductance per unit length is calculated similarly. The resistance per unit length includes the resistance of the strand and sensor wire. To calculate the resistance at high frequency, skin effects must be taken into account. The four distributed parameters are given in Table 1 (6), where a is the radius of the steel strand, b is the radius of the sensor wire, d is the center-to-center distance between the strand and wire, μ is the permeability, and ε is the permittivity.

At very high frequencies, R increases as the square root of f, whereas ωL increases directly as f, and the ratio $R/\omega L$ decreases as the square root of f. Series resistance can be neglected in the frequency range of TDR operation. For some typical values of a, b, and d (a=0.635cm, b=0.05cm, d=3.175cm), the ratio $R/\omega L$ is 1.08×10^{-2} at f=50MHz, which is negligible compared with unity; it will clearly become still more negligible at higher frequencies. $G/\omega C$ is also negligibly small, since the conductance is quite small for grout with low water content. Additionally, the sensor wire is fully insulated, which further reduces the conductance. Under these circumstances, the characteristic impedance is given to a high degree of accuracy by the simplified expression

$$Z_0 = \sqrt{\frac{R + j\omega L}{G + j\omega C}} \approx \sqrt{\frac{L}{C}}$$

Upon substituting for C and L the following expression for Z_0 results:

$$Z_0 = \frac{1}{2\pi}\sqrt{\frac{\mu}{\varepsilon}}\cosh^{-1}\left(\frac{d^2 - a^2 - b^2}{2ab}\right) \approx \frac{60}{\sqrt{\varepsilon_r}}\cosh^{-1}\left(\frac{d^2 - a^2 - b^2}{2ab}\right)$$

Note that the characteristic impedance of the line depends on the radius of the steel strand. Therefore, any physical damage to the steel strand will change the impedance. This change can be detected with TDR. More important to this work is that the impedance is also a function of ε_r, which is the dielectric constant of the surrounding material.

In the case of multiple strands, the analytical model needs to be modified. Closely spaced, electrically connected strands can be treated as a single strand with larger effective radius. The equation for characteristic impedance is still applicable, although measurement sensitivity may be affected.

Time domain reflectometry can be used to detect discontinuities in this transmission line. In a TDR test, an electrical pulse is sent along the line. It travels down the line at certain velocity determined by ε_r. When it reaches an impedance discontinuity, a reflection is generated and propagated back up the line. The impedance at the mismatch point is determined from the magnitude and phase of the reflected voltage relative to the incident voltage.

VOID DETECTION

TDR can be used as a nondestructive void detection method. This is due to the fact that a void in the grout dramatically changes the dielectric constant of the medium through which the transmission line passes, thereby affecting the characteristic impedance of the line.

To demonstrate this, five void specimens, some with multiple voids, have been fabricated and tested. Short specimens were used in the initial test for easy handling while samples with length up to 20 m were successfully monitored for corrosion in prior field demonstration (7). Thin-walled hollow balls of different diameters were used to create voids that extend across a single, 7-wire strand with a length of 1 m, a diameter of 12.77 mm, and a yield value of 1860 MPa. Holes with the same diameter as the strand were drilled in the balls on opposite sides, and the strand was passed through the holes. The openings were sealed with silicon sealant to prevent water and grout from getting into the void. The voids were located one-third of the way down the strand. Figure 3 shows the bare strand with the 5.6-cm rubber ball prior to grouting. The strand and void assembly was then placed in a 10-cm-diameter polyvinylchloride (PVC) duct and filled with grout. To increase the applicability of the laboratory testing, a typical grout used in cable-stayed bridges was used. After some initial TDR tests, a hole was drilled on the side of the specimen to provide access to the void. The properties of the void were studied, and a set of electrochemical corrosion experiments was conducted in the void. All specimens have indicated that TDR is able to detect the built-in voids. Experimental results from two specimens, which are listed in Table 2, under different test conditions are reported in this paper.

The laboratory experiments focused on voids that extend across the strand, since this type of void leaves the strands most susceptible to corrosion. Voids far away from the strand/wire transmission line might be difficult to detect due to their negligible effect on the line impedance. However, these voids are of less concern and will be the focus of future studies.

Figure 4 shows the TDR result from void specimen 1. Note that the diameter of the spherical void is 5.6 cm, which corresponds to 31% of the cross-sectional area of the duct. As stated before, the characteristic impedance of the line depends on e_r. Since $e_{r\ concrete} > e_{r\ air}$, an electrical discontinuity is introduced by the void.

In evaluating the signal produced by TDR and shown in Figure 4, it is useful to understand the setup and operation of the test. The specimen was connected to a TDR measuring system through a short section of coaxial cable. The TDR system generated a fast-rising step pulse at t=1ns. The pulse was launched into the coaxial cable, whose characteristic impedance is 50Ω. At t=9 ns, the pulse reached the connection between the coaxial cable and the specimen (marker: start). Since the connection itself was a discontinuity, a reflection was recorded there. The reflection at 13 ns was caused by the void (marker: void), and the step at 20 ns corresponded to the end of the specimen (marker: end). Note that all the times mentioned here are roundtrip times. One can see that the location of the void is easily determined based on the travel time. In this case, the total roundtrip travel time along the strand is 11 ns, while it is only 4 ns to the void. This would indicate that the void is 4/11 or 36% of the way down the strand (close to the one-third location).

Sensitivity to Void Size

Figure 5 shows a TDR reading from void specimen 2, which has a 3.7-cm void (14% of the total area of the duct). Clearly, the reflection magnitude is related to void size: a larger void tends to generate a bigger reflection. Larger voids can significantly alter the localized effective dielectric constant and therefore introduce relatively large electrical discontinuities. Even though the reflection is relatively small for this void size, it is still distinguishable.

Ideally, there is a limit to the size of voids that can be detected. Depending on the background noise level and equipment used, voids smaller than a certain size will not detectable. This practical size limitation can only be determined once a field-implementable prototype is identified.

Effect of Void Contents on Reflection

The reflection magnitude is also related to the content of the void, since different materials have different electrical properties. Different mediums were placed into the void through a hole drilled on the side of the specimen. Figure 6 shows the TDR return from specimen 1 when the void was filled with dry sand. Basically, it has a very similar shape and magnitude as the signal shown in Figure 4, which was taken while the void was filled with air. This is the case because the dielectric constant of dry sand is very close to 1, the dielectric constant of air. As close as the two signals are, changes in waveform can still be recognized from a differential comparison with Figure 4, which is also shown in Figure 6. Once the concrete specimen is instrumented, TDR readings should be repeatable, since the material and geometrical parameters that affect transmission line properties will remain unchanged. Although some noise will be present in all measurements, this noise is generally due to imperfections in the physical nature of the system, and do not change over time. As such, a differential comparison of stored signals with newly measured ones will cancel out the noise and reveal changes that occurred between the two measurements. If the change is caused by corrosion or voids, a localized, sharp discrepancy is expected. On the other hand, changes in ambient conditions such as moisture content in the grout will tend to shift the entire TDR curve slightly. The shifted curve will not show signs of localized discontinuities and can be easily distinguished from localized changes caused by corrosion or voids. The difference between an air-filled void and a sand-filled void is small but detectable. While filled with sand, the void gives off a slightly smaller reflection.

Dry porous grouts are expected to have electrical properties similar to those of sand-filled voids. The result in Figure 6 indicates that a region of chalky and porous grout can be detected by TDR. This is of practical importance, since highly porous grouts can also seriously reduce the corrosion protective capabilities of the grout.

Next, the content of the void was changed from air to water. In this case, the TDR reflection from the void changed substantially, as shown in Figure 7. While the electrical property of water is much different from air, demonstrated by the comparison with Figure 4, it is very similar to the surrounding wet concrete. For this reason, only a negligible reflection was detected at the void site.

In the above void detection tests, a steel strand was used as a part of the transmission line to enable future corrosion monitoring for the strand. However, this is not necessary; if the purpose of the nondestructive evaluation is void detection only, a section of standard transmission line, such as the inexpensive 300Ω television cable, can be used. The cable needs to be run inside the duct, and recent experiments indicate that this approach can give better results than the steel strand/wire line, since a standard transmission line is used. Any void close to the line can be easily detected. Signal deviation introduced by the transition from coaxial cable to the strand, as seen in Figures 4 through 8, can be eliminated. This allows for the detection of voids in the vulnerable anchor region since reflections from voids would not be masked by the disturbance near the interface.

One may combine this method with corrosion detection by applying a two-wire transmission line alongside the steel cable. Voids are detected by TDR on this two-wire line, while corrosion damage is detected using either one of the two wires with the steel cable. Note that shielded transmission lines such as coaxial cables are not suitable for this purpose, since their electric field is confined and does not extend into the grout.

CORROSION IN THE VOID

Typically, voids in the surrounding grout will not change the strength of the reinforcing cable. However, their presence can greatly reduce the corrosion protective capacities of the system and leave sections of the cable vulnerable to corrosion. The TDR method can not only detect the existence of voids but also monitor the corrosion progress in the void.

A set of electrochemical corrosion experiments was conducted with the void specimen. Saturated NaCl solution was added to the void. A piece of copper strip was inserted through the hole into the void. The steel strand was connected to the anode of a constant-current source while the copper strip was connected to the cathode. To expedite the corrosion process, a relatively large current of 2A was used. Several TDR readings taken over time are shown in Figure 8. Note that the void was drained and dried before each measurement to simulate the process of moisture accumulation and depletion in the void. The reflections at around 13 ns were generated from the corrosion site. The reflection magnitude increased gradually as the electrochemical corrosion continued. The extent of damage was controlled by the corrosion time and current. The TDR measurements clearly show the increase in corrosion. More details regarding the corrosion tests are given by Liu. (8).

CONCLUSIONS

Time domain reflectometry can be utilized as a novel nondestructive evaluation technique for grouted post-tensioned bridge ducts. An analytical model was developed, which represents the steel strand as an asymmetric two-wire transmission line by introducing an insulated conductive sensor alongside a steel strand. TDR is capable of detecting both corrosion and voids. The effectiveness of TDR as a void detection method was demonstrated through tests on specimens with built-in voids. Several factors affecting void detection were identified. Among them are void size, void content, and corrosion. The ability to monitor the progression of electrochemical corrosion inside of a void by TDR is also shown. Additional research is required to implement this void detection technique in the field. Future research will also focus on the possibility of using TDR on existing structures.

REFERENCES

1. Bungey, J.H., S. G. Millard, and M. R. Shaw, (1997). “Radar Assessment of Post-Tensioned Concrete,” *Proceedings of Structural Faults & Repair ’97*, Edinburgh, Scotland, 1997, pp. 331-339.

2. Shaw, J.D.N and J. Keble, J. “Durable Grouted Post-Tensioned Bridges Development of a Special Grout,” *Proceedings of Structural Faults & Repair '97*, Edinburgh, Scotland, 1997, pp. 295-298.

3. Corven Engineering. “Mid-Bay Bridge: Post-Tensioning Evaluation,” Florida Department of Transportation, Draft Report, February 8, 2001.

4. “Time Domain Reflectometry Theory.” *Hewlett-Packard Application Note 1304-2*, Hewlett-Packard Company, Palo Alto, Calif., 1998.

5. Bhatia, S. K., R. G. Hunsperger, and M. J. Chajes. “Modeling Electromagnetic Properties of Bridge Cables for Non-destructive Evaluation.” *Proc. of Int. Conference on Corrosion and Rehabilitation of Reinforced Concrete Structures*, Orlando, Florida, 1998.

6. Liu, W., R. G. Hunsperger, K. J. Folliard, M. J. Chajes, and E. Kunz. “Detection and Characterization of Corrosion of Bridge Cables by Time Domain Reflectometry,” *Proceedings of SPIE*, vol. 3587, 1999, pp 28-39, Newport Beach, Calif.

7. Liu, W., R. G. Hunsperger, M. J. Chajes, D. Li, and E. Kunz. “Nondestructive Corrosion Monitoring of Prestressed HPC Bridge Beams Using Time Domain Reflectometry,” *Proc. of TRB 80th Annual Meeting*, Washington, DC, 2001.

8. Liu, W. “Electromagnetic Modeling of Embedded Metallic Structures for Nondestructive Evaluation Using Time Domain Reflectometry,” PhD dissertation, University of Delaware, 2001.

LIST OF FIGURES AND TABLES

Figures

Tables

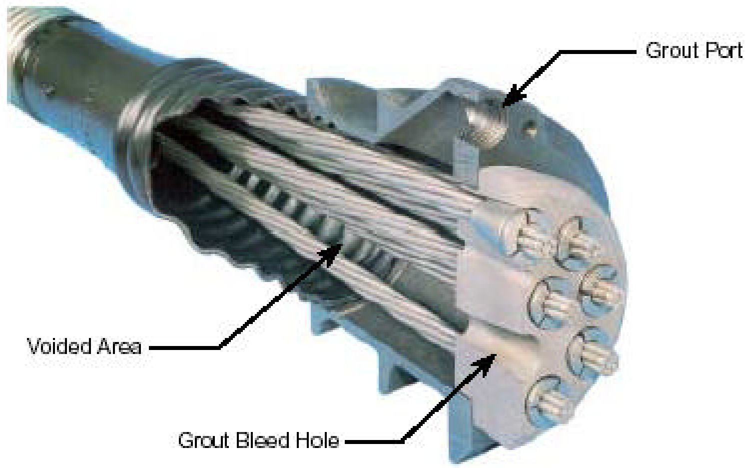

FIGURE 1 Typical Post-Tensioning Tendon Anchor with Void (3).

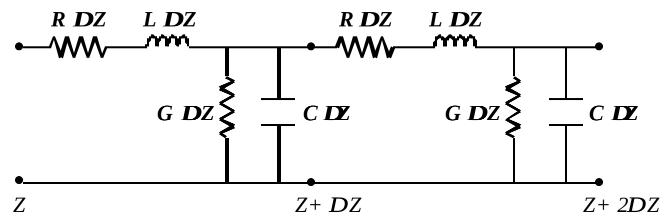

FIGURE 2 Distributed parameter equivalent circuit for the steel cable transmission line.

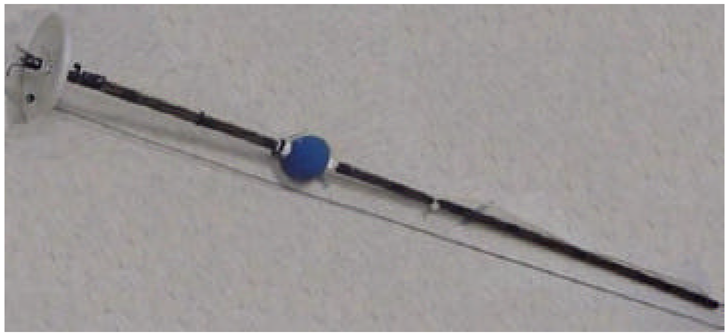

FIGURE 3 Fabrication of a Void Specimen, with a Rubber Ball Used to Simulate a Void.

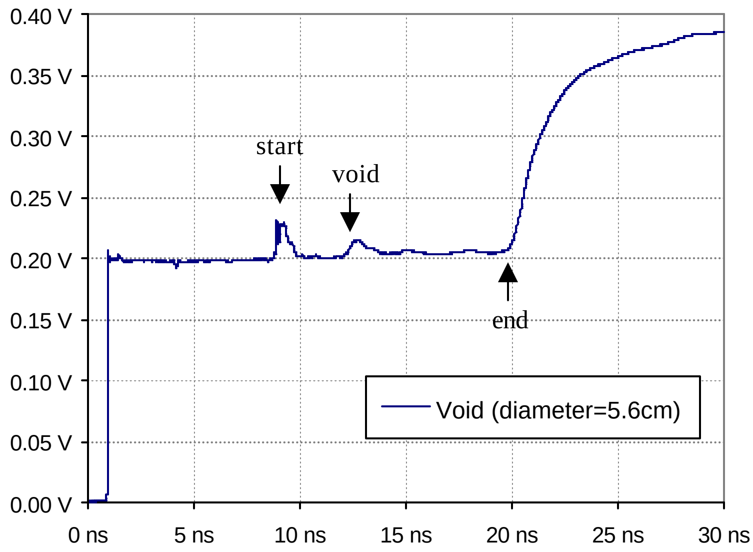

FIGURE 4 TDR Reflection from a 1-meter Specimen with Built-in Void (Specimen 1). The Reflection at 13ns is Due to the Presence of a Void.

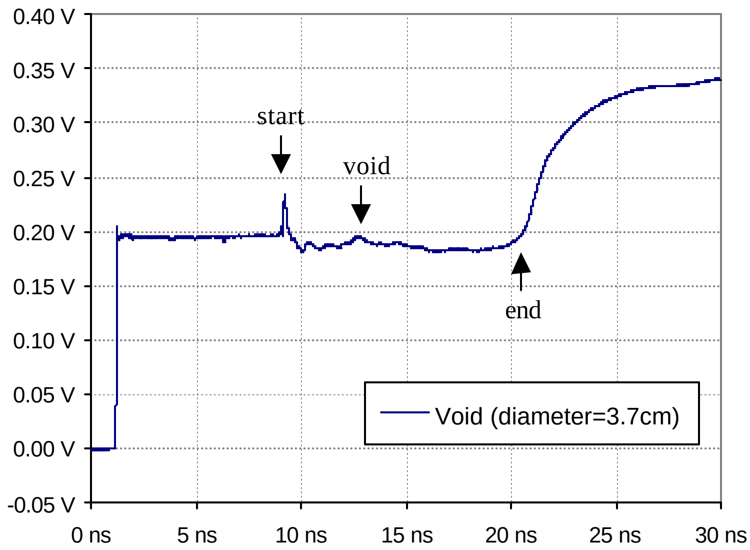

FIGURE 5 TDR Reflection from a 1-Meter Specimen (Specimen 2), which Has a Smaller Void than Specimen 1.

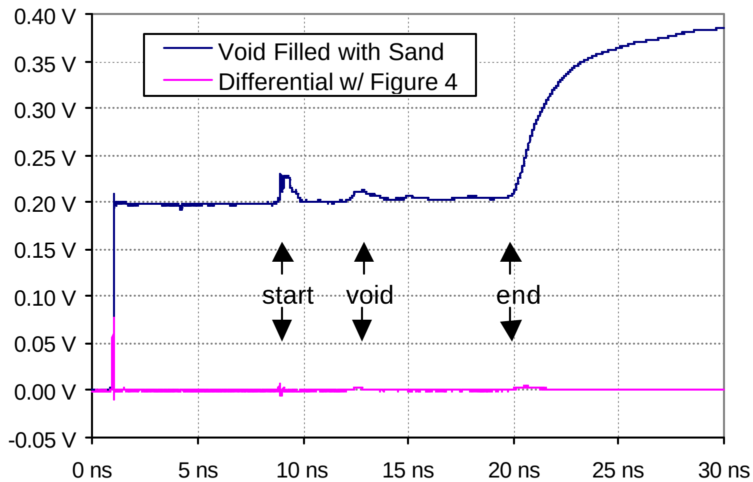

FIGURE 6 TDR Return from a Void Sample (Specimen 1) When the Void Was Filled with Sand.

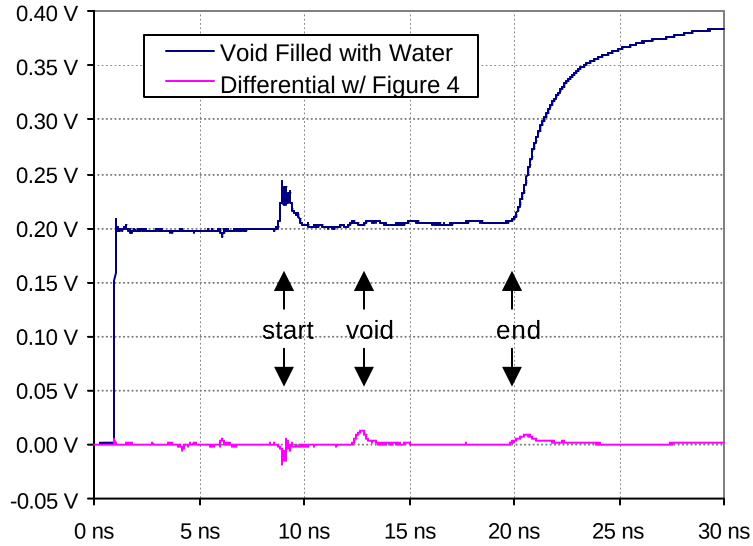

FIGURE 7 TDR Return from a Void Sample (Specimen 1) When the Void Was Filled with Water.

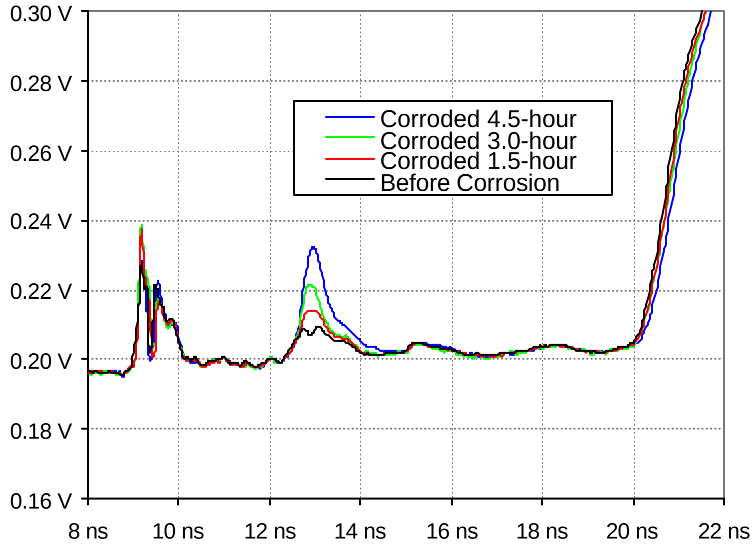

FIGURE 8. TDR Readings from Specimen 1 During the Progress of Electrochemical Corrosion.

TABLE 1 Distributed Parameters of the Steel Cable Transmission Line.

Distributed Parameters	Two-wire Transmission Line
shunt capacitance C	$C = \dfrac{2pe}{\cosh^{-1}\left(\dfrac{d^2 - a^2 - b^2}{2ab}\right)}$
series inductance L	$L = \dfrac{m}{2p}\cosh^{-1}\left(\dfrac{d^2 - a^2 - b^2}{2ab}\right)$
series resistance R	$R = \sqrt{\dfrac{fm}{4p}}\left(\dfrac{1}{a\sqrt{s_a}} + \dfrac{1}{b\sqrt{s_b}}\right)$
shunt conductance G	G is negligible for insulated sensor wire in dry grout

TABLE 2 Two Void Specimens Used in the Experimental Study.

Specimen	Length	Diameter	Void		
			Position	Diameter	Percentage of cross-sectional area at maximum
1	100 cm	10 cm	33 cm	5.6 cm	31%
2	100 cm	10 cm	36 cm	3.7 cm	14%